9-2015

Molecular View Modeling of Atmospheric Organic Particulate Matter: Incorporating Molecular Structure and Co-Condensation of Water

James F. Pankow
Portland State University, pankowj@pdx.edu

Marguerite Colasurdo Marks
Portland State University, margueritemarks@gmail.com

Kelley C. Barsanti
Portland State University, barsanti@pdx.edu

Abdullah Mahmud
Texas A & M University - College Station

William E. Asher
Portland State University

Citation Details

Pankow, J.F., Marks, M.C., Barsanti, K.C., Mahmud, A., Asher, W.E., Li, J., Ying, Q., Jathar, S.H., Kleeman, M.J., Molecular view modeling of atmospheric organic particulate matter: Incorporating molecular structure and co-condensation of water, Atmospheric Environment (2015)

Molecular View Modeling of Atmospheric Organic Particulate Matter: Incorporating Molecular Structure and Co-Condensation of Water

James F. Pankow[1,2 *], Marguerite C. Marks[2], Kelley C. Barsanti[2], Abdullah Mahmud[2], William E. Asher[2], Jingyi Li[3], Qi Ying[3], Shantanu H. Jathar[4], and Michael J. Kleeman[4]

[1]Department of Chemistry &
[2]Department of Civil & Environmental Engineering
Portland State University
Portland, Oregon 97207-0751

[3]Department of Civil Engineering
Texas A&M University
College Station, TX 77843-3136

[4]Civil and Environmental Engineering
University of California
Davis California 95616-8734

*Corresponding Author
James F. Pankow
pankowj@pdx.edu

Revised
September 4, 2015

ABSTRACT

Most urban and regional models used to predict levels of organic particulate matter (OPM) are based on fundamental equations for gas/particle partitioning, but make the highly simplifying, anonymized-view (AV) assumptions that OPM levels are not affected by either: a) the molecular characteristics of the condensing organic compounds (other than simple volatility); or b) co-condensation of water as driven by non-zero relative humidity (RH) values. The simplifying assumptions have allowed parameterized chamber results for formation of secondary organic aerosol (SOA) (e.g., "two-product" (2p) coefficients) to be incorporated in chemical transport models. However, a return towards a less simplistic (and more computationally demanding) molecular view (MV) is needed that acknowledges that atmospheric OPM is a mixture of organic compounds with differing polarities, water, and in some cases dissolved salts. The higher computational cost of MV modeling results from a need for iterative calculations of the composition-dependent gas/particle partition coefficient values. MV modeling of OPM that considered water uptake (but not dissolved salts) was carried out for the southeast United States for the period August 29 through September 7, 2006. Three model variants were used at three universities: CMAQ-RH-2p (at PSU), UCD/CIT-RH-2p (at UCD), and CMAQ-RH-MCM (at TAMU). With the first two, MV structural characteristics (carbon number and numbers of functional groups) were assigned to each of the 2p products used in CMAQv.4.7.1 such that resulting predicted $K_{p,i}$ values matched those in CMAQv.4.7.1. When water uptake was allowed, most runs assumed that uptake occurred only into the SOA portion, and imposed immiscibility of SOA with primary organic aerosol (POA). (POA is often viewed as rather non-polar, while SOA is commonly viewed as moderately-to-rather polar. Some runs with UCD/CIT-RH-2p were used to investigate the effects of POA/SOA miscibility.) CMAQ-RH-MCM used MCM to generate oxidation products, and assumed miscibility of SOA and POA. In a ~500 km wide band from

Louisiana through to at least North Carolina, CMAQ-RH-2p and UCD/CIT-RH-2p predicted that water uptake can increase SOA levels by as much as 50 to 100% (from a range of ~1 to 2 μg m^{-3} to a range of ~1 to 4 μg m^{-3}). CMAQ-RH-MCM predicted much lower effects of water uptake on SOA levels (<10% increase). The results from CMAQ-RH-2p and UCD/CIT-RH-2p are considered more reflective of reality. In the Alabama/Georgia hotspot, both CMAQ-RH-2p and UCD/CIT-RH-2p predicted aerosol water levels that are up to nearly half the predicted SOA levels, namely ~0.5 to 2 μg m^{-3}. Such water levels in SOA will affect particle optical properties, viscosity, gas/particle partitioning times, and rates of hydrolysis and water elimination reactions.

Keywords: organic particulate matter, OPM, organic aerosol, OA, secondary organic aerosol, SOA, absorption model, RH effects, water, co-condensation of water

■ INTRODUCTION

Most current 3D chemical transport models use primitive approaches for predicting levels of organic particulate matter (OPM) in the atmosphere: they incorporate only the barest aspects of the chemistry of the complex mixes of organic compounds that may occur, ignore the role of co-condensing water, and usually do not attempt to consider the time-dependent oxidation reactions that continually transform organic compounds in the atmosphere. This is problematic: 1) aerosol particles are known to have direct and indirect effects on climate (Ramanathan et al., 2001; Kanakidou et al., 2005); 2) ambient levels of fine PM are associated with increases in human morbidity and mortality (Pope and Dockery, 2006); and 3) atmospheric PM is often 20 to 60% organic material (Kanakidou et al., 2005). In those contexts, the composition of the OPM can strongly affect light absorption (Andreae and Gelencsér, 2006; Updyke et al. 2012; and Song et al., 2013), cloud condensation (Petters and Kreidenweis, 2007), and particle deposition rates (composition affects hygroscopicity (Petters and Kreidenweis, 2007) and hygroscopicity affects deposition rates (Vong et al., 2010)).

While views vary regarding the advantages and deficiencies of different modeling approaches, there is scientific consensus at least that in the general case: 1) a portion of ambient OPM has some volatility, and so is in active evaporation/condensation (*i.e.*, gas/particle) exchange with the gas phase; and 2) a second portion is essentially non-volatile at the ambient temperature *T*. Both the exchanging and non-volatile fractions can be subdivided as anthropogenic or biogenic, and further as primary (directly emitted) or secondary. For a neutral species, an inherently low volatility is always ascribable to the combined effects of molecular weight (MW), polarity, and temperature *T*. Temperature plays its role through vapor pressure, which sets the volatility for every particular pure liquid compound *i*. Atmospheric OPM, however, is never a single pure compound, so the effective volatility of each constituent

105 compound is lowered by dilution, and changed by non-ideal solution effects (Pankow, 1994a).
106 Regarding acidic and basic species i.e. organic carboxylic acids can be deprotonated to form
107 carboxalate ions, and organic amines can be protonated to form aminium ions, charge alone is
108 enough to prevent volatilization at ambient *T* values (*cf*. protonation of ammonia to form
109 ammonium ion) (Pankow, 2003).

110 Chemical transport models in current use for atmospheric OPM modeling such as CMAQ
111 and PMCAMx (Carlton et al., 2010; Robinson et al., 2007) suffer from two deficiencies that
112 affect OPM predictions. *First*, they both utilize a severely *anonymized view* (AV) in which a
113 limited number (20 or less) of "hypothetical lumped compounds" is invoked. The "compounds"
114 vary only by inherent volatility, with no other characteristics such as polarity. Examples of the
115 AV approach include the two-product (2p) view of Odum et al. (1996, 1997) as used in CMAQ
116 (Carlton et al., 2010), and the 1-D volatility basis set (VBS) of Donahue et al. (2006). In fact,
117 contrary to the AV assumption, both low polarity and polar constituents are always present in
118 atmospheric OPM, and those differences will affect the levels and properties of the OPM. Low
119 polarity constituents include plant wax materials, cooking oils, and petroleum hydrocarbons
120 (Schauer et al., 1999; Schauer et al., 2002; Conte and Weber, 2002); polar constituents include
121 secondary compounds with functional groups such as hydroxyl and carboxyl (e.g., Yu et al.,
122 1999; Zhang et al., 2007). Each OPM phase will therefore be a mix with a mixture-average
123 polarity that is between non-polar and highly polar. For each exchanging compound *i*, the
124 gas/particle partitioning is affected by the polarity match or mismatch in the liquid between the
125 compound and the OPM mixture. A high mismatch (relative to condensation into a liquid in
126 which $\zeta_i = 1$) causes $\zeta_i > 1$ which reduces the condensation tendency (*viz*. increases the
127 volatility) (Pankow, 1994a; Pankow, 2003). When the condensed material includes both non-
128 polar and rather polar compounds in similar abundance, phase separation in the OPM becomes

129 certain (Erdakos and Pankow, 2004; Zuend et al., 2010; Donahue et al., 2011), as when within
130 the miscibility gap of a partially miscible binary system. While anonymized models ignore these
131 complexities, a *molecular view* (MV) can assign functionalities to each OPM compound to allow
132 consideration of non-ideality effects, and phase separation.

133 *Second*, AV modeling precludes consideration of water uptake: there is no character of
134 the OPM that can be used to estimate hygroscopicity. However, theory (e.g., Pankow, 1994a;
135 Pankow, 2010; Pankow and Chang, 2008; Chang and Pankow, 2010), and applications with the
136 3D sesqui-MADRID model (Pun, 2008), predict that important effects on OPM levels are
137 possible. Indeed, although water is far more volatile than "condensable" organic compounds, it
138 is also always vastly more abundant in the atmosphere than the sum of all condensable organic
139 compounds (~10^7 $\mu g/m^3$ water at 20 ^oC, 50% relative humidity (RH), and 1 atm total pressure).
140 In addition to the importance of the effects of water on OPM levels and that of hygroscopicity
141 itself (e.g., Massoli et al., 2010, Duplissy et al. 2011), there are expected significant effects of
142 absorbed water on viscosity (Iwata and Shimada, 2013) and thus gas/particle equilibration times
143 (Shiraiwa et al., 2011; Bones et al., 2012), and reaction rates within organic liquids (Vollhardt
144 and Schore, 2007). Fortunately, once an adequately flexible MV model is built for considering
145 compounds with varying polarity and molecular weight, inclusion of water as a fully-interacting
146 partitioning compound is simple. With the 2-D VBS of Donahue et al. (2011), while some
147 measure of MV effects amongst the partitioning organic compounds can be considered, only O:C
148 ratio and carbon number are available as measures of molecular variability, and water is not
149 included in the basis set so it cannot be predicted to be present in, or have an effect on the levels
150 of, the modeled OPM. We are interested in modeling carried out considering specific
151 functionalities (alcohol groups, aldehyde groups, carboxylic acid groups, etc.) assigned to
152 partitioning organic molecules, and allowing water uptake.

153 Herein we provide an overview of the OPM model development required for a simple
154 consideration of MV effects for non-ionic organic compounds, with water uptake into a single
155 OPM phase; the effects of ionization and multiple OPM phases (i.e., phase separation) are
156 beyond the scope of this work. Simulations are described for the southeast United States for the
157 period August 29 through September 7, 2006 using three chemical transport models modified to
158 include MV features for OPM calculations. The implications of water uptake for OPM phase
159 characteristics are considered.

160 ## ■ EQUILIBRIUM GAS/PARTICLE PARTITIONING - EQUATIONS AND SOLUTIONS

161 **General.** The gas/particle partitioning constant for compound *i* is defined

162 $$K_{p,i}\ (\mathrm{m^3\ \mu g^{-1}}) \;=\; \frac{c_{p,i}}{c_{g,i}} \quad (\equiv 1/C_i^*) \tag{1}$$

163 where $c_{p,i}$ (μg μg^{-1}) is the concentration within the particle phase, and $c_{g,i}$ (μg m^{-3}) ($\equiv A_i$) is the
164 concentration in the gas phase. In the 1-D "volatility basis set" (VBS) approach of Donahue et
165 al. (2006), $K_{p,i}$ is manifested in terms of the saturation concentration C_i^* (μg m^{-3}). If the total
166 mass concentration of the absorbing phase is M (μg m^{-3}), and F_i (μg m^{-3}) is the particle-
167 associated concentration of *i* for the aerosol system, then (Pankow, 1994a)

168 $$K_{p,i}\ (\mathrm{m^3\ \mu g^{-1}}) \;=\; \frac{F_i / M}{A_i} \tag{2}$$

169 $$F_i \;=\; K_{p,i} M\ A_i \tag{3}$$

170 As usual, let T_i (μg m^{-3}) = $A_i + F_i$ be the total (*i.e.*, gas+particle) concentration of *i*, and the
171 fraction of *i* in the particle phase is

172 $$f_{p,i} \;\equiv\; \frac{F_i}{F_i + A_i} = \frac{K_{p,i} M}{1 + K_{p,i} M} \tag{4}$$

173 $$M \;=\; \sum\nolimits_i F_i \;=\; \sum\nolimits_i f_{p,i} T_i \;=\; \sum\nolimits_i \frac{K_{p,i} M}{1 + K_{p,i} M}\ T_i \tag{5}$$

$$1 - \sum_i \frac{K_{p,i} T_i}{1 + K_{p,i} M} = 0 \qquad (6)$$

When water is considered, M includes a contribution from water because F_w is one of the F_i, and M here equals M_{o+w} as used elsewhere (Pankow, 2010). In the case of some essentially non-volatile component i, the value of $K_{p,i}$ is very large so that $f_{p,i} = 1.0$.

For $M > 0$, the function represented by the left hand side of Eq.(6) is a smooth sigmoidal curve. As M increases from 0, the curve varies from $(1 - \sum_i K_{p,i} T_i)$ to 1. If $\sum_i K_{p,i} T_i > 1$, then the function will be negative at very small M, and there will be an easily found zero crossing (i.e., a solution), which gives the condition at which the multi-component system is saturated in the gas phase with material left over for $M > 0$. With $K_{p,i}$ as the inverse of the saturation concentration C_i^*, for a single component system $K_{p,1} T_1$ gives the ratio between the total and saturation concentrations, so that $M > 0$ only when $K_{p,1} T_1 > 1$.

Mathematical Solution in the Anonymized View (AV). In AV models of OPM, at a particular value of T, the $K_{p,i}$ values are fixed and not dependent on OPM composition. As noted, associated options include: a) the 2p model of Odum et al. (1996, 1997) for condensation of "secondary" organic aerosol (SOA) compounds; and b) the 1-D-VBS approach of Donahue et al. (2006) for general OPM modeling. Given input sets of T_i and the associated $K_{p,i}$, a root solver with Eq.(6) can find the root value of M such that the left hand side equals zero. The root value of M can then be used to calculate each F_i by Eq.(3). CMAQv.4.7.1 uses this approach with 2p values of $K_{p,i}$ (chamber-derived) for assumed oxidation products of several SOA parent hydrocarbons. Note that: a) low values of the T_i and/or $K_{p,i}$ can cause there to be no real positive root value for M in Eq.(6), in which case $M = 0$; but b) if $T_i > 0$ for any species considered to be non-volatile, $M > 0$ regardless of the values of the other T_i and $K_{p,i}$.

196 **Mathematical Solution in the Molecular View (MV).** The MV approach is needed because
197 $K_{p,i}$ values depend on OPM composition. For absorptive partitioning into liquid OPM (Pankow,
198 1994a):

199 $$K_{p,i} = \frac{RT}{10^6 \, \overline{MW} \, \zeta_i \, p^o_{L,i}} \quad (7)$$

200 where: R = gas constant (8.2×10^{-5} m^3 atm mol^{-1} K^{-1}); $\overline{MW}$ (g mol^{-1}) = mole-average mole-
201 cular weight of the absorbing OPM phase; ζ_i (dimensionless) = mole-fraction scale activity
202 coefficient; and $p^o_{L,i}$ (atm) = vapor pressure at temperature T (K) of pure liquid i. (The factor 10^6
203 is a conversion factor that gives the number of μg per gram.) For reference, if the OPM were
204 pure liquid i, then $\overline{MW} = MW_i$ $\zeta_i = 1$, $c_{p,i} = 1$, and C^*_i gives the gas-phase saturation
205 concentration in equilibrium with the pure liquid.

206 The compositional dependence of $K_{p,i}$ is caused by variability in: a) ζ_i, which accounts
207 for the comfort match/mismatch between i in *its own liquid self* vs. in *the OPM*, as due to
208 differences in characteristics such as polarity and size; and b) $\overline{MW}$, which accounts for the
209 colligative consequences of $MW_i \neq \overline{MW}$. Because of the low MW of water (18 g mol^{-1}), water
210 absorption by OPM can cause marked reductions in $\overline{MW}$, which can cause every $K_{p,i}$ to
211 increase. For example, absorption by dry OPM with $\overline{MW}$ = 200 g mol^{-1} of 2% by weight water
212 lowers $\overline{MW}$ to 167 g mol^{-1}, tending to cause all $K_{p,i}$ values to increase by 20%. When OPM
213 levels are low and most of the potentially condensable organic material is in the gas phase, the
214 predicted OPM level at equilibrium is very sensitive to even relatively minor changes in the $K_{p,i}$
215 and T_i values (Pankow, 2010, 2013).

216 In an MV modeling approach, the partitioning compounds have differentiating structural
217 features, and the equilibrium composition can only be obtained by the coupled iterative solution

of Eq.(7) for all *i* together with Eq.(6) (Pankow, 1994b). A $K_{p,i}$ algorithm first takes guess values of F_i (*i.e.*, the OPM guess composition) to compute the corresponding guess values of all the ζ_i and $\overline{MW}$, and thus the $K_{p,i}$ values for that composition based on Eq.(7). As discussed above, if $\Sigma_i K_{p,i} T_i > 1$, an OPM root solver with Eq.(6) can use the $K_{p,i}$ values and the guess M ($=\Sigma_i F_i$) to easily obtain a new M, which can be used with Eq.(4) to obtain the new F_i. Iterative alternation between the $K_{p,i}$ algorithm and the OPM root solver continues until convergence is obtained (as evaluated by examination of either: 1) the $K_{p,i}$; or 2) the F_i). When phase separation is not being considered, we have not experienced difficulties obtaining convergence because of local minima. Oscillation during the alternation between the two solutions may occur at low OPM levels, but is increasingly dampened when "non-volatile" components contribute significantly, and/or predicted OPM levels are large relative to the condensable mass: the mathematical sensitivity is dampened as each particular $T_i > 0$ is consigned to the OPM phase (common in current modeling), and when M is large relative to the condensable mass (Pankow, 2013).

■ METHODS: THREE MOLECULAR VIEW-ENABLED MODELS

Models. Table 1 summarizes details of the three chemical transport models used here for MV consideration of OPM levels; all consider water uptake into OPM. For each: 1) an iterative solution was begun at each point in the *x,y,z,t* domain using the $K_{p,i}$ algorithm with the local RH and *T*, guess values of the F_i, and the UNIFAC model (Fredenslund et al., 1977), to calculate corresponding guess of ζ_i and $\overline{MW}$ and the resulting $K_{p,i}$; 2) the $K_{p,i}$ are passed to an OPM root solver; 3) iteration proceeds until convergence is reached. CMAQ-RH-2p was derived from CMAQv.4.7.1 (an AV model) by addition of two features: a) $K_{p,i}$ algorithm; and b) an input array (for each 2p product) for values of the numbers of particular functional groups and the MW. The values for the MV characteristics array for each product (summarized in Table 2) were ob-

tained along with the carbon number n_C using the approach of Chang and Pankow (2010) such that the utilized values of MW_i and $p^{o}_{L,i}$ (T = 298 K, by SIMPOL.1 (Pankow and Asher, 2008)) for the product gave a $(K_{p,i})^{-1}$ value that closely matches the C^{*}_{i} value used in CMAQv.4.7.1. UCD/CIT-RH-2p employs the two features and corresponding code that CMAQ-RH-2p adds to CMAQv.4.7.1, but is otherwise based on the UCD/CIT model (Kleeman et al., 2001; Ying et al., 2008). UCD/CIT uses an updated secondary organic aerosol module based on CMAQv.4.7.1, but does not consider SOA production by in-cloud processes. CMAQ-RH-MCM is based on MCM-SOA (Li et al., 2015), but adds water uptake into the OPM (MCM-SOA provided the first adaptation of CMAQ for MV consideration of SOA formation using a $K_{p,i}$ algorithm, employing UNIFAC for the latter). MCM-SOA uses the near-explicit chemical reaction model MCM.3.2 (Jenkin et al., 2012) to produce oxidation products available for condensation of SOA. For each time step, values are initialized using the values produced by the preceding step. None of the models considered partitioning to mostly-water phases, so Henry's Law partition coefficients for water were not used. For all three models, the spatial resolution was 36 km; operator splitting time steps were between 6 and 10 min.

Runs. Averaged model output for the southeast United States was obtained for the 10 day period August 29 through September 7, 2006, with 1 to 5 *preceding* days of model "spin-up". For each model, the base (B) case run assumed no water uptake by the OPM; for each model water (W) mode run was also carried out, with water uptake allowed into the SOA as determined at each point (x,y,z,t) according to the local conditions. All runs with CMAQ-RH-2p imposed immiscibility of SOA with primary organic aerosol (POA) (POA is often viewed as rather non-polar, while SOA is commonly viewed as moderately-to-rather polar); CMAQv.4.7.1 assumes POA/SOA miscibility. When water uptake was allowed in CMAQ-RH-2p, it was

assumed that uptake occurred only into the SOA portion. UCD/CIT-RH-2p was executed similarly, except that some runs allowed POA/SOA miscibility with water uptake into the mixture. CMAQ-RH-MCM assumes POA/SOA miscibility with water uptake into the mixture.

■ RESULTS AND DISCUSSION

Model results are presented in Figures 1 and 2. In Figure 1, the first and second (a and b) panel columns indicate that both CMAQ-RH-2p and UCD/CIT-RH-2p predict that water uptake can significantly increase average SOA levels in areas of the southeast United States during the model period, from a range of ~1 to 2 $\mu g\ m^{-3}$ to a range of ~1 to 4 $\mu g\ m^{-3}$**.** While the results of Pun (2008) for July 2, 2002 for this region using sesqui-MADRID indicate significantly higher SOA levels, the corresponding percentage increases due to water uptake are similar. The most affected region in Figure 1 is a ~500 km wide band from Louisiana through to about Virginia. The mostly modest differences between the results from CMAQ-RH-2p and UCD/CIT-RH-2p are consistent with the differences between the two models: 1) gas-phase mechanisms used (SAPRC07, Carter (2010) *vs*. SPARC11, Carter (2013)); 2) meteorology algorithm used (MM5 with nudging as described by Ngan et al. (2012) vs. WRFv.3.4 (WRF, 2014) with the NAM reanalysis data set); and 3) imposed limit (for model stability) on input RH values assumed for water uptake (99% *vs*. 95%). Given the fact that RH values approaching 100% require amounts of condensed water that are large relative to any expected ambient OPM levels, model instability at RH ≈ 100% is to be expected in any model that considers co-condensation of water. ζ_i values for organic compounds with the MCM-SOA model have been found to be mostly in the range $0.33 < \zeta < 3$; the same was found to be true for the CMAQ-RH-2p runs carried out here, except that for the SQT species values as large as 40 were often calculated. For the CMAQ-RH-2p runs, $\zeta_{water} \approx 1$, due to the hydrophilicity of polar functional groups on the SOA species.

Runs carried out using UCD/CIT-RH-2p allowing miscibility of the SOA and POA and therefore water uptake into the total OPM did not significantly change the predicted levels of SOA or associated water. In contrast to the results with CMAQ-RH-2p and UCD/CIT-RH-2p, CMAQ-RH-MCM resulted in lower predicted increase in the levels of SOA because CMAQ-RH-MCM forms mostly non-volatile SOA (which is not directly sensitive to RH effects). This is consistent with the conclusions of others that MCM generally cannot explain observed ambient OPM levels without arbitrary downward adjustment of the vapor pressures of semivolatile products (Johnson et al, 2006), or by including other SOA generation pathways such as formation of non-volatile products by reactive surface uptake (Li et al,, 2015), as implemented here in CMAQ-RH-MCM (see Figure 2).

The fourth column of panels in Figure 1 summarizes the findings for predicted water uptake effects on SOA levels. For CMAQ-RH-2p and UCD/CIT-RH-2p, fractional increases as large as 0.5 to 1.0 and higher (50 to 100% and higher) are indicated. Much weaker effects are predicted for CMAQ-RH-MCM. The levels of water predicted to be present in the OPM for the water uptake runs are given in Figure 1. In the Alabama/Georgia hotspot, CMAQ-RH-2p and UCD/CIT-RH-2p give predicted organic aerosol water levels of ~0.5 to 2 $\mu g\ m^{-3}$, nearly half their predicted levels of SOA. The water levels predicted by CMAQ-RH-MCM are substantially lower, and a consequence of the typically large estimated water activity coefficients in the modeled OPM.

The CMAQ-RH-2p and UCD/CIT-RH-2p results may be more indicative of reality in this region than those from CMAQ-RH-MCM, with the latter providing a lower limit estimation of the SOA water effect. Consistent with our results are the indirectly measured particle water levels reported by Guo et al. (2015) for the southeast United States. At four sites (three urban and one rural) in Alabama and Georgia in 2012 (May through November), Guo et al. (2015)

report that OPM-associated water was “significant”, averaging 29 to 39% of all particle water. Also, the OPM-associated water values were found to be correlated with the organic mass fraction, and with RH.

Significant levels of water in OPM carry considerable importance for understanding the levels and properties atmospheric OPM. First, the viscosity of many organic liquids decreases strongly with increasing water content (*e.g.*, Acierno and Van Puyvelde, 2005), and decreasing OPM viscosity facilitates gas/particle equilibration. Second, water content will affect the OPM phase polarity, and liquid phase polarity affects reaction rates (much current discussion of OPM formation processes involves condensed phase reactions). Third, the activity of water within an OPM phase will obviously directly affect the rates of reactions that involve water, *e.g.*: a) hemiacetal to acetal conversion (Jang and Kamens, 2001); b) organic ester and amide formation Barsanti and Pankow, 2006); and c) sulfate ester formation (Surratt et al.,2007, 2008). Fourth, particle water at levels as high as 10 $\mu g\ m^{-3}$ in the southeast US and formed by condensation on atmospheric sulfate has been proposed by Carlton and Turpin (2013) as an important compartment for the uptake from the gas phase of water soluble organic compounds (*e.g.*, glyoxal (C_2), methyl glyoxal (C_3), and higher carbon number compounds). However, uptake of such molecules into water-rich OPM would compete non-negligibly with uptake into sulfate-associated particle water, especially when electrolyte concentrations are high (Zuend and Seinfeld, 2012).

Overall, despite the model improvements discussed in this work, the predictive modeling carried out here unquestionably still suffers greatly from many simplistic assumptions, *e.g.*, the limited volatility range of the assumed 2p products, and the absence of a progression of second, third, and higher generation products. Nevertheless, the results demonstrate that an MV approach with water uptake is required when modeling OPM in the atmosphere.

■ ACKNOWLEDGMENTS

The Portland State University authors acknowledge financial support from the Electric Power Research Institute, the Cooley Family Fund for Critical Research of the Oregon Community Foundation, the Institute for Sustainable Solutions of Portland State University, and the Murdock Charitable Trust (for support of the Gaia computing cluster). The authors at University of California at Davis acknowledge support from the California Air Resources Board (Contract # 11-755). The authors at Texas A&M University thank the Texas A&M Supercomputing Facility (http://sc.tamu.edu) and the Texas Advanced Computing Center (http://www.tacc.utexas.edu/) for providing essential computing resources.

■ REFERENCES

Acierno, S., Van Puyvelde, P., 2005. Rheological behavior of polyamide 11 with varying initial moisture content. Journal of Applied Polymer Science 97, 666–670.

Andreae, M.O., Gelencsér, A. 2006. Black carbon or brown carbon? The nature of light-absorbing carbonaceous aerosols, Atmospheric Chemistry and Physics 6, 3131–3148.

Baltaretu, CO., Lichtman, E.I., Hadler, A.B., Elrod, M.J., 2009. Primary atmospheric oxidation mechanism for toluene. Journal of Physical Chemistry A 113, 221-230.

Barsanti, K.C., Pankow, J.F., 2006. Thermodynamics of the formation of atmospheric organic particulate matter by accretion reactions. 3. Carboxylic and dicarboxylic acids. Atmospheric Environment 40, 6676-6686.

Bones, D.L., Reid, J.P., Lienhard, D.M., Krieger, U.K., 2012. Comparing the mechanism of water condensation and evaporation in glassy aerosol. Proceedings of the National Academy of Sciences of the USA 109, 11613-11618.

Calvert, J.G., Atkinson, R., Becker, K.H., Kamens, R.M., Seinfeld, J.H., Wallington, T.J., Yarwood, G., 2002. *The Mechanisms of Atmospheric Oxidation of the Aromatic Hydrocarbons*, Oxford University Press, Oxford, 566 pp.

Carlton, A.G., Bhave, P.V., Napelenok, S.L., Edney, E.D.; Sarwar, G., Pinder, R.W., Pouliot, G.A., Houyoux, M., 2010. Model representation of secondary organic aerosol in CMAQv4.7. Environmental Science and Technology 44, 8553-8560.

Carlton, A.G., Turpin, B.J., 2013. Particle partitioning potential of organic compounds is highest in the Eastern US and driven by anthropogenic water. Atmospheric Chemistry and Physics 13, 10203–10214.

Carter, W.P.I., 2010. SAPRC-07 mechanism. http://www.engr.ucr.edu/~carter/SAPRC/. Accessed November 18, 2014.

371 Carter, W.P.I., 2013. Revised version of SAPRC-11 mechanism. 2013.
372 http://www.engr.ucr.edu/~carter/SAPRC/. Accessed November 18, 2014.
373 Chang, E.I., Pankow, J.F., 2010. Organic particulate matter formation at varying relative
374 humidity using surrogate secondary and primary organic compounds with activity
375 corrections in the condensed phase obtained using a method based on the Wilson equation.
376 Atmospheric Chemistry and Physics 10, 5475–5490.
377 Conte, M.H., Weber, J.C., 2002. Plant biomarkers in aerosols record isotopic discrimination of
378 terrestrial photosynthesis. Nature 417, 639-641.
379 Donahue, N.M., Robinson, A.L., Stanier, C.O., Pandis, S.N., 2006. Coupled partitioning,
380 dilution, and chemical aging of semivolatile organics. Environmental Science and Technology
381 40, 2635-2643.
382 Donahue, N.M., Epstein, S.A., Pandis, S.N., Robinson, A.L., 2011. A two-dimensional volatility
383 basis set: 1. organic-aerosol mixing thermodynamics. Atmospheric Chemistry and Physics
384 11, 3303–3318.
385 Duplissy, J., DeCarlo, P.F., Dommen, J., Alfarra, M.R., Metzger, A., Barmpadimos, I., Prevot,
386 A.S.H., Weingartner, E., Tritscher, T., Gysel, M., Aiken, A.C., Jimenez, J.L., Canagaratna,
387 M.R., Worsnop, D.R., Collins, D.R., Tomlinson, J., Baltensperger, U., 2011. Relating
388 hygroscopicity and composition of organic aerosol particulate matter, Atmospheric Chemistry
389 and Physics 11, 1155-1165.
390 Erdakos, G.B., Pankow, J.F., 2004. Gas/particle partitioning of neutral and ionizing compounds
391 to single and multi-phase aerosol particles. 2. Phase separation in liquid particulate matter
392 containing both polar and low-polarity organic compounds. Atmospheric Environment 38,
393 1005-1013.

394 Fredenslund, A., Gmehling, J., Rasmussen, P., 1977. *Vapor–Liquid Equilibria Using UNIFAC:*
395 *A Group Contribution Method*. Elsevier, Amsterdam, 380 pp.
396 Guo, H., Xu, L., Bougiatioti, A., Cerully, K.M., Capps, S.L., Hite, J.R., Carlton, A.G., Lee, S.-
397 H., Bergin, M.H., Ng, N.L., Nenes, A., Weber, R.J., 2015. Fine-particle water and pH in
398 the southeastern United States. Atmospheric Chemistry and Physics 15, 5211–5228.
399 Iwata, H., Shimada, K., 2013. *Formulas, Ingredients and Production of Cosmetics*, XII, 224 p.
400 Springer-Verlag GmbH, Heidelberg.
401 Jang, M., Kamens, R.M., 2001. Atmospheric secondary organic aerosol formation by
402 heterogeneous reactions of aldehydes in the presence of sulfuric acid aerosol catalyst.
403 Environmental Science and Technology 35, 4758-4766.
404 Jenkin, M.E., Wyche, K.P., Evans, C.J., Carr, T., Monks, P.S., Alfarra, M.R., Barley, M.H.,
405 McFiggans, G.B., Young, J.C., Rickard, A.R., 2012. Development and chamber
406 evaluation of the MCM v3.2 degradation scheme for β-caryophyllene. Atmospheric
407 Chemistry and Physics 12, 5275-5308.
408 Johnson, D., Utembe, S.R., Jenkin, M.E., Derwent, R.G., Hayman, G.D., Alfarra, M.R., Coe, H.,
409 McFiggans, G. (2006) Simulating regional scale secondary organic aerosol formation
410 during the TORCH 2003 campaign in the southern UK. Atmospheric Chemistry and
411 Physics 6, 403-418.
412 Kanakidou, M., Seinfeld, J.H., Pandis, S.N., Barnes, I.; Dentener, F.J., Facchini, M.C., Van
413 Dingenen, R., Ervens, B., Nenes, A., Nielsen, C.J., Swietlicki, E., Putaud, J.P., Balkanski, Y.,
414 Fuzzi, S., Horth, J., Moortgat, G.K., Winterhalter, R., Myhre, C.E.L., Tsigaridis, K., Vignati,
415 E., Stephanou, E.G., Wilson, J., 2005. Organic aerosol and global climate modeling: a review.
416 Atmospheric Chemistry and Physics 5, 1053-1123.

417 Kleeman, M.J., Cass, G.R., 2001. A 3D Eulerian source-oriented model for an externally mixed
418 aerosol. Environmental Science and Technology 35, 4834-4848.
419 Li, J., Cleveland, M., Ziemba, L., Griffin, R.J., Barsanti, K.C., Pankow, J.F., Ying, Q., 2015.
420 Modeling regional secondary organic aerosol using the master chemical mechanism.
421 Atmospheric Environment (in press).
422 Massoli, P., Lambe, A.T., Ahern, A.T., Williams, L.R., Ehn, M., Mikkilä, J., Canagaratna, M. R.,
423 Brune, W.H., Onasch, T.B., Jayne, J.T., Petäjä, T., Kulmala, M., Laaksonen, A., Kolb, C.E.,
424 Davidovits, P., Worsnop, D.R., 2010. Relationship between aerosol oxidation level and
425 hygroscopic properties of laboratory generated secondary organic aerosol (SOA) particles,
426 Geophysical Research Letters 37, L24801.
427 Ngan, F., Byun, D., Kim, H., Lee, D, Rappengluck, B., Pour-Biazar, A., 2012. Performance
428 assessment of retrospective meteorological inputs for use in air quality modeling during
429 TexAQS 2006. Atmospheric Environment 54, 86-96.
430 Odum, J.R., Hoffmann, T., Bowman, F., Collins, D., Flagan, R.C., Seinfeld, J.H., 1996.
431 Gas/particle partitioning and secondary organic aerosol yields. Environmental Science and
432 Technology 30, 2580–2585.
433 Odum, J.R., Jungkamp, T.P.W., Griffin, R.J., Flagan, R.C., Seinfeld, J.H., 1997. The
434 atmospheric aerosol-forming potential of whole gasoline vapor. Science 276, 96-99.
435 Pankow, J.F., 1994a. An absorption-model of gas-particle partitioning of organic-compounds in
436 the atmosphere. Atmospheric Environment 28, 185-188.
437 Pankow, J.F., 1994b. An absorption model of the gas/aerosol partitioning involved in the
438 formation of secondary organic aerosol. Atmospheric Environment 28, 189-193.

439 Pankow, J.F., 2003. Gas/particle partitioning of neutral and ionizing compounds to single and
440 multi-phase aerosol particles. 1. Unified modeling framework. Atmospheric Environment 37,
441 3323-3333.
442 Pankow, J.F., Asher, W.E., 2008. SIMPOL.1: A simple group contribution method for
443 predicting vapor pressures and enthalpies of vaporization of multifunctional organic
444 compounds. Atmospheric Chemistry and Physics 8, 2773–2796.
445 Pankow, J.F., Chang, E.I., 2008. Variation in the sensitivity of predicted levels of atmospheric
446 organic particulate matter (OPM). Environmental Science and Technology 42, 7321-7329.
447 Pankow, J.F., 2010. Organic particulate material levels in the atmosphere: Conditions favoring
448 sensitivity to varying relative humidity and temperature. Proceedings of the National
449 Academy of Sciences of the USA 107, 6682-6686.
450 Pankow, J.F., 2013. Equations for the sensitivity of the equilibrium mass concentration of
451 organic particulate matter with respect to changes in ambient parameters: A technical note.
452 Atmospheric Environment 64, 374-379.
453 Petters, M.D., Kreidenweis, S.M. 2007. A single parameter representation of hygroscopic
454 growth and cloud condensation nucleus activity. Atmospheric Chemistry 7, 1961–1971.
455 Pope, C.A., Dockery, D.W., 2006. Health effects of fine particulate air pollution: lines that
456 connect. Journal of the Air and Waste Management Association 56, 709-742.
457 Pun, B.K. 2008. Development and initial application of the sesquiversion of MADRID. Journal
458 of Geophysical Research 113, D12212.
459 Ramanathan, V.;,Crutzen, P.J., Kiehl, J.T., Rosenfeld, D., 2001. Atmosphere - aerosols, climate,
460 and the hydrological cycle. Science 294, 2119-2124.

461 Robinson, A.L., Donahue, N.M., Shrivastava, M.K., Weitkamp, E.A., Sage, A.M., Grieshop,
462 A.P., Lane, T.E., Pierce, J.R., Pandis, S.N., 2007. Rethinking organic aerosols: semivolatile
463 emissions and photochemical aging. Science 315, 1259-1262.
464 Sato, K., Takami, A., Kato, Y., Seta, T., Fujitani, Y., Hikida, T., Shimono, A., Imamura, T.,
465 2012. AMS and LC/MS analyses of SOA from the photooxidation of benzene and 1,3,5-
466 trimethylbenzene in the presence of NOx: effects of chemical structure on SOA aging.
467 Atmospheric Chemistry and Physics 12, 4667-4682.
468 Schauer, J.J., Kleeman, M.J., Cass G.R., Simoneit, B.R.T., 1999. Measurement of emissions
469 from air pollution sources. 2. C1 through C30 organic compounds from medium duty diesel
470 trucks. Environmental Science and Technology 33, 1578-1587.
471 Schauer, J.J., Kleeman, M.J., Cass, G.R., Simoneit, B.R.T., 2002. Measurement of emissions
472 from air pollution sources. 5. C1−C32 organic compounds from gasoline-powered motor
473 vehicles. Environmental Science and Technology 36, 1169–1180.
474 Shiraiwa, M., Ammann, M., Koop, T., Poschl, U., 2011. Gas uptake and chemical aging of
475 semisolid organic aerosol particles. Proceedings of the National Academy of Sciences of the
476 USA 108, 11003-11008.
477 Smith, D.F., Kleindienst, T.E., McIver, C.D., 1999. Primary product distributions from the
478 reaction of OH with *m*-, *p*-xylene, 1,2,4- and 1,3,5-trimethylbenzene. Journal of
479 Atmospheric Chemistry 34, 339-364.
480 Song, C., Gyawali, M., Zaveri, R.A. Shilling, J.E., Arnott, W.P., 2013. Light absorption by
481 secondary organic aerosol from α-pinene: Effects of oxidants, seed aerosol acidity, and
482 relative humidity. Journal of Geophysical Research – Atmospheres 118, 11,741–11,749.
483 Surratt, J.D., Murphy, S.M., Kroll, J.H., Ng, N.L., Hildebrandt, L., Sorooshian, A., Szmigielski,
484 R., Vermeylen, R., Maenhaut, W., Claeys, M., Flagan, R.C., Seinfeld, J.H., 2006.

485 Composition of secondary organic aerosol formed from the photooxidation of isoprene**.**
486 Journal of Physical Chemistry A 110, 9665–9690.
487 Surratt, J.D., Kroll, J.H., Kleindienst, T.E., Edney, E.O., Claeys, M., Sorooshian, A., Ng, N.L.,
488 Offenberg, J.H., Lewandowski, M., Jaoui, M., Flagan, R.C., Seinfeld, J.H., 2007.
489 Evidence for organosulfates in secondary organic aerosol. Environmental Science and
490 Technology 41, 517–527.
491 Surratt, J.D., Gómez-González, Y., Chan, A.W.H., Vermeylen, R., Shahgholi, M., Kleindienst,
492 T.E., Edney, E.O., Offenberg, J.H., Lewandowski, M., Jaoui, M., Maenhaut, W., Claeys,
493 M., Flagan, R.C., Seinfeld, J.H., 2008. Organosulfate formation in biogenic secondary
494 organic aerosol. Journal of Physical Chemistry A 112, 8345–8378.
495 Updyke, K.M., Nguyen, T.B., Nizkorodov, S.A.,2012. Formation of brown carbon via reactions
496 of ammonia with secondary organic aerosols from biogenic and anthropogenic
497 precursors. Atmospheric Environment 64, 22-31.
498 Vollhardt, K.P.C., Schore, N.E., 2007. *Organic Chemistry: Structure and Function*, 5th Ed.,
499 W.H. Freeman Co, New York, NY, 1369 pp.
500 Vong, R.J., Vong, I.J., Vickers, D., Covert, D.S. Size-dependent aerosol deposition velocities
501 during BEARPEX'07. Atmospheric Chemistry and Physics 10, 5749–5758.
502 Warscheid, B., Hoffmann, T., 2001. Structural elucidation of monoterpene oxidation products by
503 ion trap fragmentation using on-line atmospheric pressure chemical ionisation mass
504 spectrometry in the negative ion mode. *Rapid Commun. Mass Spec.* **2001** *15*, 2259-2272.
505 WRF: The Weather Research & Forecasting Model. WRFv3.4 http://www.wrf-model.org.
506 Accessed November 21, 2014.
507 Ying, Q., Lu, J., Allen, P., Livingstone, P., Kaduwela, A., Kleeman, M.J., 2008. Modeling air
508 quality during the California Regional PM10/PM2.5 Air Quality Study (CRPAQS) using the

509 UCD/CIT source-oriented air quality model - Part I. Base case model results. Atmospheric
510 Environment 42, 8954-8966.
511 Yu, J., Cocker, D.R., Griffin, R.J., Flagan, R.C., Seinfeld, J. H., 1999. Journal of Atmospheric
512 Chemistry 34, 207-258.
513 Zhang, Q., Jimenez, J.L., Canagaratna, M.R., Allan, J.D., Coe, H., Ulbrich, I., Alfarra, M.R.,
514 Takami, A., Middlebrook, A.M., Sun, Y.L., Dzepina, K., Dunlea, E., Docherty, K., DeCarlo,
515 P. F., Salcedo, D., Onasch, T., Jayne, J.T., Miyoshi, T., Shimono, A., Hatakeyama, S.,
516 Takegawa, N., Kondo, Y., Schneider, J., Drewnick, F., Borrmann, S., Weimer, S., Demerjian,
517 K., Williams, P., Bower, K., Bahreini, R., Cottrell, L., Griffin, R.J., Rautiainen, J., Sun, J.Y.,
518 Zhang, Y.M., Worsnop, D.R., 2007. Ubiquity and dominance of oxygenated species in
519 organic aerosols in anthropogenically-influenced Northern Hemisphere midlatitudes.
520 Geophysical Research Letters 34, L13801.
521 Zuend, A., Marcolli, C., Peter, T., Seinfeld, J.H., 2010. Computation of liquid-liquid equilibria
522 and phase stabilities: implications for RH-dependent gas/particle partitioning of organic-
523 inorganic aerosols. Atmospheric Chemistry and Physics 10, 7795–7820.
524 Zuend, A., Seinfeld, J.H., 2012. Modeling the gas-particle partitioning of secondary organic
525 aerosol: the importance of liquid-liquid phase separation. Atmospheric Chemistry and
526 Physics 12, 3857–3882.
527

528 Figure Captions

529

530 Figure 1. 10-day averaged output in the surface layer from three molecular view-enabled
531 chemical transport models for August 29 through September 7, 2014 (after 1 to 5 days of
532 model spin-up). Surface layer = 0 to 34 m for PSU and TAMU, 0 to 50 m for UCD. For
533 CMAQ-RH-2p and UCD/CIT-RH-2p results, SOA and POA assumed immiscible; for
534 CMAQ-RH-MCM, SOA and POA assumed miscible. Base (B) case runs: **a.** Secondary
535 organic aerosol (SOA) levels with no water uptake. With water (W) uptake runs: **b.** SOA
536 levels as determined at each point (*x*,*y*,*z*,*t*) according to the local RH; **c.** Particle-phase water
537 levels within the OPM; and **d.** Fractional increases in predicted SOA levels as compared to
538 the base (B) case (no water uptake).
539

540 Figure 2. Stacked bar graphs for POA (primary organic aerosol), anthropogenic SOA (secondary
541 organic aerosol), biogenic SOA, and water (in OPM) for models run at PSU (CMAQ-RH-
542 2p), UCD (UCD/CIT-RH-2p), and TAMU (CMAQ-RH-MCM). Results are 10-day
543 averaged output in the surface layer for August 29 through September 7, 2014 (after 1 to 5
544 days of model spin-up). Surface layer = 0 to 34 m for PSU and TAMU, 0 to 50 m for UCD;
545 SOA and POA assumed immiscible. The base (B) case runs assumed no water uptake. For
546 the PSU and UCD runs, the with water (W) uptake runs assumed water co-condensation into
547 the SOA only as determined at each point (*x*,*y*,*z*,*t*) according to the local RH. For the TAMU
548 runs, the W runs assumed water co-condensation into the mixed SOA+POA at each point
549 (*x*,*y*,*z*,*t*) according to the local RH.
550

Table 1. Details for Three Applications of Chemical Transport Models in a Molecular View (MV) of Secondary Organic Aerosol (SOA) Formation with Water Uptake.

Common features across the applications:

a) emissions: anthropogenic inputs generated from the 2005 National Emission Inventory (NEI); biogenic inputs generated using the Biogenic Emissions Inventory, Version 3 (BEIS3); all inputs processed using the Sparse Matrix Operator Kernal Emission (SMOKE) model;

b) condensed compounds: SOA compounds are formed by initial reaction of volatile organic compounds (VOCs); some of the SOA material is assumed to become non-volatile, as assumed in CMAQ 4.7.1; POA inputs are considered non-volatile for all model time, as assumed in CMAQ 4.7.1;

c) water: RH > 0 causes water uptake into OPM;

d) activity coefficients: composition-dependent ζ_i values in the absorbing phase are calculated using UNIFAC.

Application (SOA framework, and gas phase chemical mechanism)	Molecular view (MV) of Condensed SOA and POA			
	SOA semi-volatile portion	SOA non-volatile portion	POA	Characteristics of OPM Phase(s)
CMAQ-RH-2p[a] (CMAQ 4.7.1[b], with AERO5 and SAPRC07)	1. Structural features (carbon number n_C and numbers of functional groups) assigned to the 12 hypothetical, 2p type products in CMAQ 4.7.1 for oxidation of seven hydrocarbon SOA precursors; 2. The structural features of each product chosen so that the predicted K_p value matched the K_p value used in CMAQ 4.7.1 for 298 K (see Table 2); 3. Dependence of K_p on T computed as in CMAQ 4.7.1.	1. Structural features (carbon numbers and numbers of functional groups) assigned to six of the hypothetical non-volatile lumped products assumed by CMAQ 4.7.1 to form via oxidation pathways starting in the gas-phase: three products for the direct oxidation of aromatic SOA precursors via the low-NOx pathway; one accretion (aka "oligomer") product from aging[c] of condensed anthropogenic SOA products; one accretion product from aging of biogenic SOA products; one product from the acid-catalyzed reaction of isoprene; 2. Assigned structural features consistent with negligible volatility under ambient conditions as well as structures reported for chamber organic particulate matter; 3. Cloud processing of gyloxyal/methylglyoxal excluded.	Retained anonymized as in CMAQ 4.7.1 because POA was assumed non-miscible with SOA (POA structures are then not needed for MV modeling of SOA).	1. Absorbing phase = non-vol. SOA + semi-vol. SOA + water; and 2. POA considered a separate phase because that is most consistent with low-polarity POA. (Unmodified CMAQ 4.7.1 simply assumes POA and SOA are miscible.)
UCD/CIT-RH-2p[d] (CMAQ 4.7.1 as deployed in UCD/CIT[e], with SAPRC11)	Same as above.	Same as above.	*option 1* POA retained anonymized as above	1. Absorbing phase = non-vol. SOA + semi-vol. SOA + water; and 2. POA non-miscible and non-sorbing.
			option 2 POA assigned a mix of four specific structures (C_{25} alkanes, levoglucosan, monoglyceride, and C_{18} acid)	Absorbing phase = all OPM + water. (POA miscible and sorbing.)
CMAQ-RH-MCM[f] (CMAQ 4.7.1 as deployed in MCM-SOA[g], with MCM)	1. The Master Chemical Mechanism (MCM) was used to generate specific condensable organic products of atmospheric oxidation as in Li et al. (2015) 2. Dependence of K_p on T computed as in Li et al. (2015)	1. Specific accretion products (aka "oligomers") were considered to form by aging[3] of the condensed-phase portions of the MCM-generated products; 2. Specific chemical structures were assumed for the non-volatile products of acid-catalyzed reaction of isoprene; 3. Specific non-volatile products were assumed for the reactive surface uptake of 1,4-dicarbonyl compounds and isoprene epoxydiol.	POA represented using a mixture of eight specific structures and assumed miscible.	Absorbing phase = all OPM + water.

[a]Runs were carried out on the “CsAR” computer cluster at PSU;

[b]Community Multi-Scale Air Quality Model, version 4.7.1, see Carlton et al. (2010);

[c]All semi-volatile products converted to non-volatile products with rate constant $k_{olig} = 9.6 \times 10^{-6}$ s^{-1};

[d]Runs were carried out on the “Wolf” computer cluster at University of California at Davis;

[e]Kleeman and Cass (2001); Ying et al. (2008);

[f]Runs were carried out on the “eos” computer cluster at the Texas A&M University, and the on the “lonestar” computing cluster in the Texas Advanced Computing Center at University of Texas as Austin.

[g]Li et al. (2015).

Table 2.a. Semi-volatile CMAQ 2p Products for Secondary Organic Aerosol (SOA) Formation with Assigned Molecular View (MV) Characteristics as Used in CMAQ-RH-2p and UCD/CIT-RH-2p.

Characteristics in CMAQ 4.7.1		vapor pressure from B (using G)	Assigned Molecular View (MV) Characteristics (D through H) (Consistent with Inferred p_L^o, as based on Pankow and Asher (2008))									
A	B	C	D	E numbers of UNIFAC groups assigned to structure to match (with n_C) the inferred p_L^o (UNIFAC group number)							F	G	H
2p product	$1/C^* = K_p$ (298 K)	inferred p_L^o (atm) (298 K)	assumed number of carbons n_C	E1 CH3 (1)	E2 CH2 (2)	E3 CH (3)	E4 OH (15)	E5 CH2CO (20)	E6 CHO (21)	E7 COOH (43)	formula	MW (g/mol)	$\frac{OM}{OC}$
ALK	50.0	2.72E-12	7	2	2	2	3	0	0	1	$C_7H_{16}O_5$	180	2.14
BNZ1	3.3	4.58E-11	5	0	0	0	0	1	1	2	$C_6H_5O_6$	161	2.68
BNZ2	9.0E-03	2.03E-08	5	1	1	1	2	0	2	0	$C_6H_{12}O_4$	134	2.23
ISO1	8.6E-03	2.15E-08	5	0	0	3	3	1	0	0	$C_5H_8O_4$	132	2.20
ISO2	1.6	1.13E-10	5	0	0	5	4	0	0	0	$C_5H_9O_4$	133	2.23
SQT	0.08	1.09E-09	15	5	4	0	0	2	2	0	$C_{15}H_{24}O_4$	273	1.52
TOL1	0.43	3.49E-10	6	1	1	1	2	1	0	1	$C_6H_{11}O_5$	163	2.26
TOL2	4.7E-02	2.97E-09	8	2	2	2	1	0	1	1	$C_8H_{15}O_4$	175	1.82
TRP1	0.13	1.03E-09	8	2	2	2	3	1	0	0	$C_8H_{17}O_4$	177	1.84
TRP2	9.0E-03	1.37E-08	9	0	1	1	0	2	3	0	$C_9H_{10}O_5$	198	1.83
XYL1	0.76	1.85E-10	6	0	0	0	0	2	0	2	$C_6H_6O_6$	174	2.42
XYL2	2.9E-02	4.55E-09	8	0	1	1	0	2	1	1	$C_8H_9O_5$	185	1.93

Table 2.b. Non-Volatile CMAQ Products from Condensed 2p Secondary Organic Aerosol (SOA) Products with Assigned Molecular View (MV) Characteristics as Used in CMAQ-RH-2p and UCD/CIT-RH-2p.

Characteristics in CMAQ 4.7.1		vapor pressure from B (using G)	Assigned Molecular View (MV) Characteristics (D through H) (Consistent with Inferred p_L^o, as based on Pankow and Asher (2008))									
A	B	C	D	E							F	G	H
				numbers of UNIFAC groups assigned to structure to match (with n_C) the inferred p_L^o (UNIFAC group number)									
non-volatile product	1/C^* = K_p [a] (298 K)	inferred p_L^o (atm) (298 K)	assumed number of carbons n_C	E1 CH3 (1)	E2 CH2 (2)	E3 CH (3)	E4 OH (15)	E5 CH2CO (20)	E6 CHO (21)	E7 COOH (43)	formula	MW[b] (g/mol)	OM/OC
BNZ3 [c]	9.7E03	1.43E-14	5	0	0	3	3	0	0	2	$C_5H_{11}O_7$	180	3.0
TOL3 [d]	2.3E04	5.39E-15	6	0	1	3	3	0	0	2	$C_6H_{10}O_7$	194	2.7
XYL3 [e]	2.0E04	1.18E-13	8	0	1	4	1	0	0	3	$C_8H_{10}O_7$	218	2.3
ISO3 [f]	5.0E04	2.32E-15	8	2	1	5	6	0	0	0	$C_8H_{19}O_6$	211	2.2
OLGA [g]	8.3E03	1.43E-14	7	0	2	2	1	0	0	3	$C_7H_{10}O_7$	206	2.5
OLGB [h]	1.3E05	7.58E-16	10	1	3	3	1	0	0	3	$C_{10}H_{16}O_7$	248	2.1

[a] At all realistic values of SOA mass concentration, these large K_p values give $f_p \approx 1$ (compound is essentially non-volatile, see Eq.(4)). These assignments are consistent with the practice in CMAQ4.7.1 of simply assigning all non-volatile SOA compounds to the particle phase, and not calculating f_p.

[b] Precedence for assigning MW was given to roughly matching the values given in CMAQ4.7.1, even though ostensibly some of the presumed non-volatile products are accretion products of some type. Little change in the simulation output would have resulted from assigning higher MW values while preserving carbon mass in the semi-volatile → non-volatile conversion step.

[c] Based roughly on a structure discussed by Sato et al. (2012).

[d] Based roughly on a structure discussed by Baltaretu et al. (2009).

[e] Roughly a dimer of a structure discussed by Smith et al. (1999).

[f] Similar to a structure discussed by Surratt et al. (2006).

[g] Roughly a dimer of a structure discussed by Calvert et al. (2002).

[h] Based on Scheme 7 of Warscheid and Hoffmann (2001).

figure 1 with all individual elements, better quality overall

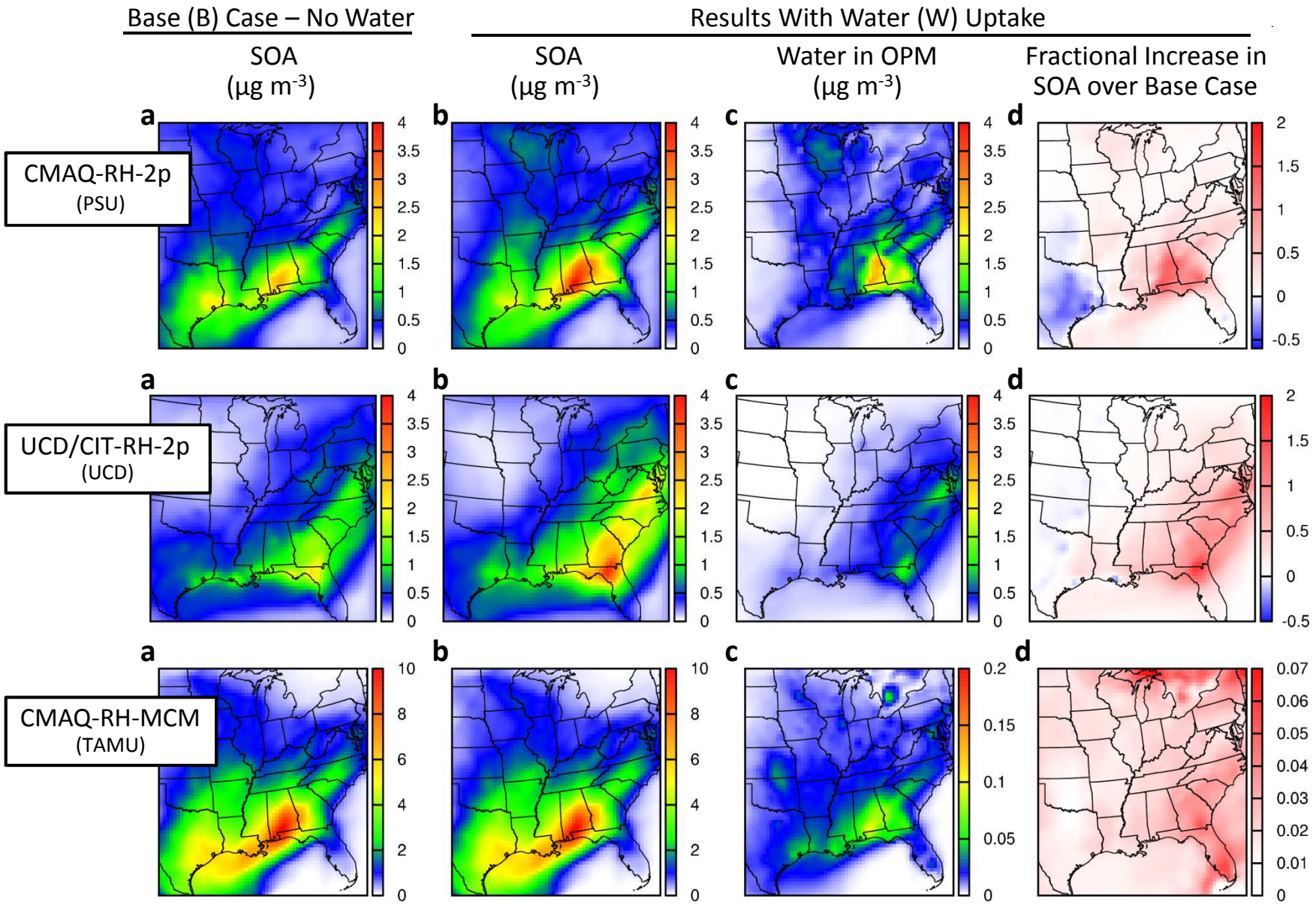

figure 1 as single image

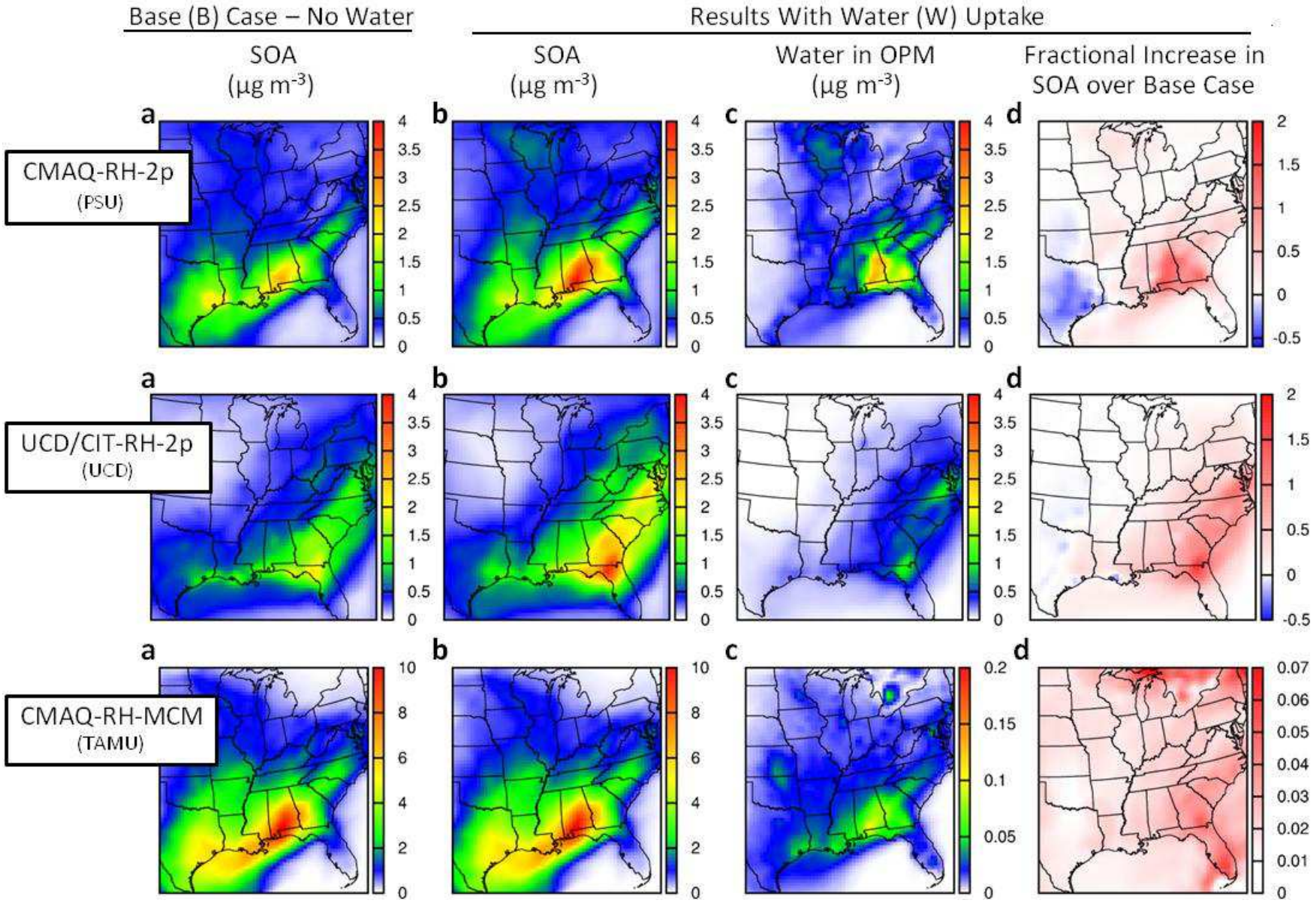

figure 2 with all individual elements, better quality overall

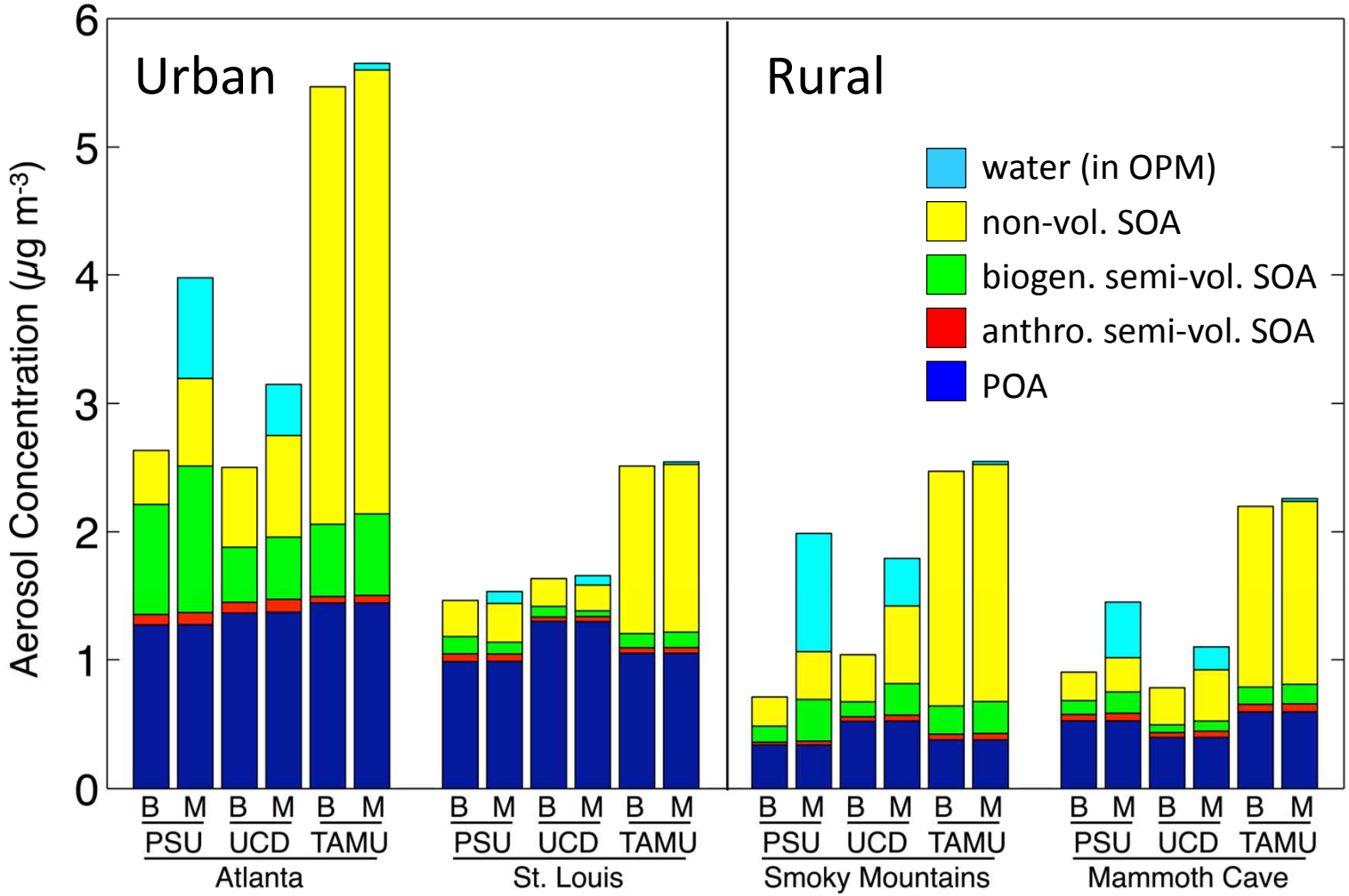

figure 2 as single image

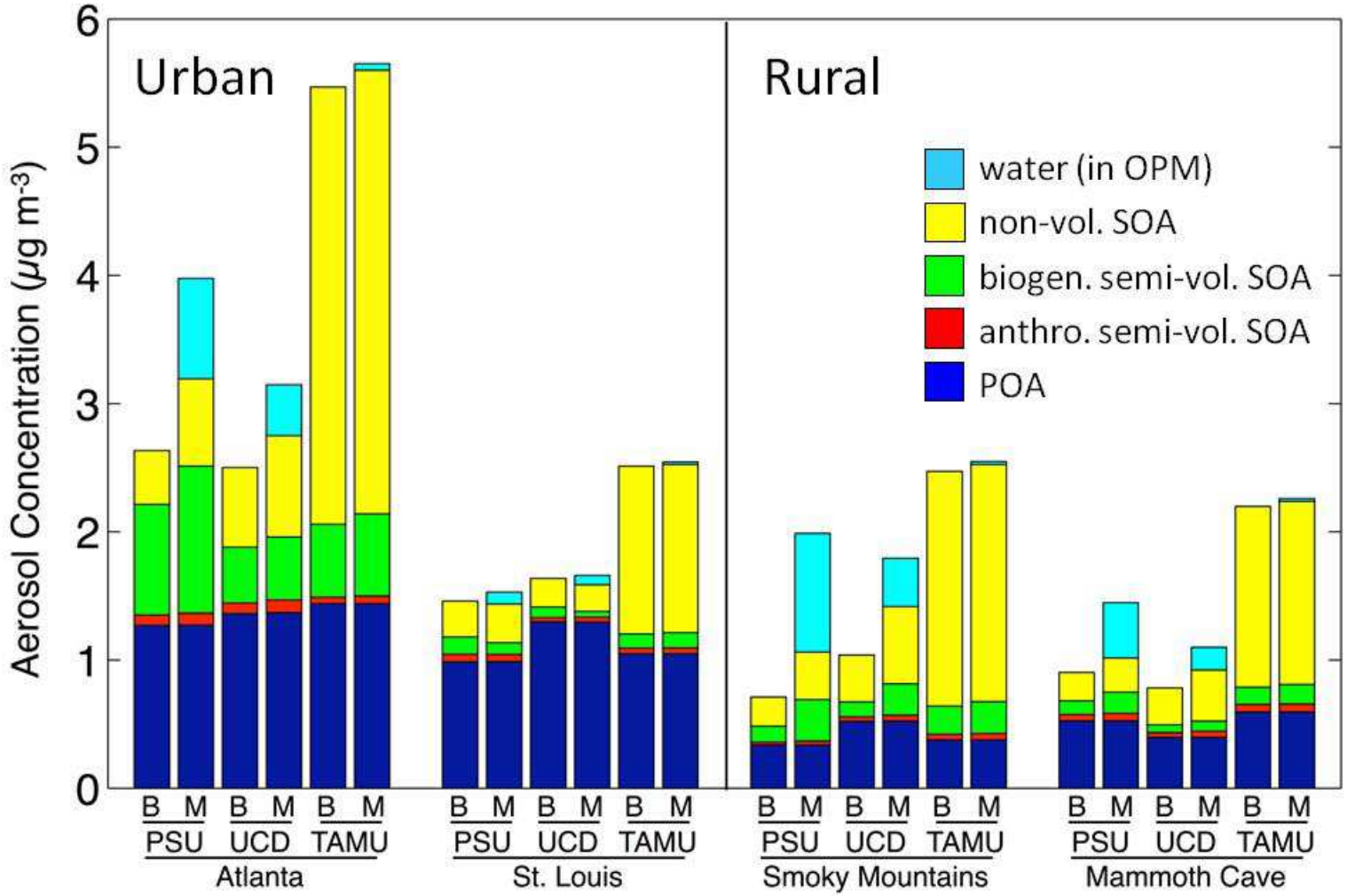

HIGHLIGHTS

- Current 3-D transport models use anonymized view modeling of organic particulate matter (OPM).
- Anonymized view modeling assigns only a volatility (vapor pressure) to each OPM constituent.
- Anonymized view modeling cannot consider effects of water uptake on OPM levels.
- Molecular view modeling assigns structural features to each OPM constituent.
- Molecular view modeling can consider effects of water uptake on OPM levels and OPM properties.